Geotechnical Testing Journal

doi:10.1520/GTJ20160284 / Vol. 41 / No. 3 / May 2018 / available online at www.astm.org

R. Matos,[1] P. Pinto,[2] C. Rebelo,[2] M. Veljkovic,[3] and L. Simões da Silva[2]

Axial Monotonic and Cyclic Testing of Micropiles in Loose Sand

Reference

Matos, R., Pinto, P., Rebelo, C., Veljkovic, M., and Simões da Silva, L., "Axial Monotonic and Cyclic Testing of Micropiles in Loose Sand," *Geotechnical Testing Journal*, Vol. 41, No. 3, 2018, pp. 526–542, https://doi.org/10.1520/GTJ20160284. ISSN 0149-6115

ABSTRACT

Micropiles, which are small-diameter deep foundation solutions with diameters that can measure up to 300 mm, are often used to reinforce new and existing foundations. Their use in the foundations of structures with high eccentricity, such as wind towers when subjected to wind loads, may lead to more efficient and economical solutions. As the new generation of wind towers will reach more than 150 m tall, very large and uneconomical gravity foundations are required. In regions of high seismicity this problem is aggravated. To evaluate the behavior of micropiles under variable loading and predict the improvement of the reinforced solution, load tests were performed on steel micropiles under controlled laboratory conditions. A total of 36 tests were conducted on 3-m-long pipe micropiles, both while isolated and in 2 by 2 groups, with three different spacings. The micropiles were installed in a cylindrical container filled with calibrated sand and tested under monotonic and cyclic loading, first without grout, then when low-pressure grouted and retested, with the aim to evaluate the improvement caused by the grout injection, the micropile spacing, and application of cyclic loading both in terms of resistance and stiffness. An improvement both in stiffness and resistance due to the grouting was obtained and, for the applied cyclic loading, there was no clear reduction in micropile cyclic stiffness. The presented results provide a tool for the calibration of numerical models to estimate the behavior of real-scale micropiles installed in higher density sand.

Keywords

micropiles, hybrid foundations, experimental tests, cyclic loading, pressure grout

Manuscript received November 7, 2016; accepted for publication September 22, 2017; published online March 22, 2018.

[1] Civil Engineering Department, University of Coimbra, Rua Luís Reis Santos, Pólo II, 3030-788 Coimbra, Portugal (Corresponding author), e-mail: ruimatos@dec.uc.pt, https://orcid.org/0000-0001-9822-8692

[2] Civil Engineering Department, University of Coimbra, Rua Luís Reis Santos, Pólo II, 3030-788 Coimbra, Portugal https://orcid.org/0000-0002-6424-8561 (P.P.)

[3] Delft University of Technology, Faculty of Civil Engineering and Geosciences, Building 23, Stevinweg 1, 2628 CN Delft, PO Box 5048, 2600 GA Delft, The Netherlands

Introduction

The latest developments of onshore wind towers will see an increase in height to improve efficiency and productivity as these towers are able to reach more stable wind profiles.

For typical shallow foundations of steel tubular towers up to 100 m high, current practice dictates that 85 % of the total weight belongs to the concrete foundation. It is expected that this percentage will increase

with tower height. One option to improve the shallow foundations is to install micropiles around the periphery of the foundation, thus increasing its tensile resistance. The main aim is to improve the overturning resistance of the tower. This solution will be more effective on foundations with higher force eccentricity, such as steel wind towers, where the vertical force is low compared to the bending moment. Concrete towers in areas of high seismicity may also benefit from this hybrid solution as concluded by Matos et al. (2016).

To analyze the improvement of a shallow foundation made by the addition of micropiles, load tests on steel pipe micropiles, installed in loose sand, were performed under controlled conditions to assess their resistance and stiffness. These tests provided a tool that can calibrate the numerical models used to estimate the behavior (resistance and stiffness) of micropiles with real-scale dimensions and installed in higher density sandy soils under similar conditions.

This article focuses on the monotonic and cyclic behavior of the tested micropiles, both when isolated and in groups, ungrouted and with pressure grout injection. The grouted micropiles in these tests present a behavior like Type A, according to Sabatini et al. (2005), because of the very low grouting pressure considered.

The first tests were carried out under monotonic loading with a constant rate of displacement until micropile failure. On subsequent tests, quasi-static load cycles were applied prior to the monotonic loading in order to check the influence of the cycle loading on the resistance and stiffness of the micropiles.

The influence of the grout injection on the resistance of the micropiles was also studied. The load tests were conducted first on ungrouted micropiles, which were subsequently injected with pressured grout and retested. It is expected that the testing sequence, with the same pile loaded before and after grouting, should have a minimal impact on the results, thus allowing the comparison presented in this paper. The reasons for this will be presented in a later section.

The effect of micropile spacing was assessed through tests performed on groups of 2 by 2 micropiles, with spacing varying from three to five pile diameters.

Background Information

The first references and studies about the use of micropiles were presented and conducted by Lizzi (1978). This small-diameter deep foundation system, with a diameter of up to 300 mm, was initially developed to strengthen old foundations but was quickly adopted as an interesting solution for a large variety of geotechnical and structural problems, with particular interest for situations with difficult access, seismic retrofit of existing structures, ground reinforcement, and structures subjected to tensile and cyclic loads. The load transfer in this system occurs mainly by side friction as the tip cross section is reduced, and the total length is commonly higher than 10 m.

Most of the experimental data available have been obtained with full-scale in situ tests, and the number of tests under laboratory conditions is reduced, especially on the scale adopted in the present work.

The most extensive work presented on the behavior of micropiles was carried out in the scope of the FOREVER project (Cyna et al. 2004). It covered full-scale prototypes, small-scale models tested under 1g (gravity acceleration) conditions, and pressure chamber and centrifuge testing.

Most of the existing tests were conducted under 1g conditions, which allows for the simulation of the micropile installation procedure and grouting conditions closer to in situ conditions, such as those performed by Russo (2004), Schwarz (2000), El Sharnouby and El Naggar (2011, 2012), and El Hadi Drbe and El Naggar (2014).

The pressure chamber tests provide a good simulation of high confining stresses, as is found in longer micropiles, but these stresses were almost constant along the micropile length (Francis 1997; Le Kouby 2003; Boulon and Foray, cited by Cyna et al. 2004; Juran and Weinstein 2009). Even though centrifuge testing allows the simulation of the installation procedure and higher confining stresses, which increase with depth, it is still very difficult to properly simulate the grouting process (Juran, Benslimane, and Hanna 2001; Alnuaim, El Naggar, and El Naggar 2015a, 2015b, 2016).

The resistance and stiffness behavior of micropile foundations depend on a number of factors. The most influential are the ground type, the installation process, the micropile geometry (diameter and length), reinforcement, pile spacing, and the loading conditions.

The type of soil, such as sand, clay, or rock, influences the behavior of the micropiles in terms of lateral and tip resistance. Francis (1997) and Le Kouby (2003) evaluated the behavior of small-scale micropiles (single and groups) installed in sand and concluded that the most representative parameters for the evaluation of the cyclic behavior of the elements are the displacement amplitude, the loading sequence, and the installation mode.

Cyna et al. (2004) showed in their study under the scope of the FOREVER project that the shaft resistance is largely dependent on the soil grain size, besides the expected influence of the surface rugosity. The ground properties also influence the micropile behavior, and, in sand, the static stiffness and limit load increase with the density index.

These deep foundation elements are sensitive to the installation type and injection procedure. The use of grout allows a considerable improvement on the micropile resistance because of the increase in the micropile/ground interface shear resistance and the increase in the friction surface (increase in the diameter) of the element.

Grouting may be performed under gravity pressure (Type A), through the casing under low pressure, typically from 0.5 to 1 MPa (Type B), low pressure followed by a single high-pressure phase (Type C or Injection Globale Unitaire (IGU)) or by multiple high-pressure phases (Type D or Injection Répétitive et Séléctive (IRS)). The value for the unit shaft resistance is higher for IRS than for IGU according to the charts presented by Bustamante and Doix (1985) and the values provided by Sabatini et al. (2005), which are corroborated by Russo (2004), who obtained values for the unit shaft resistance of 95 kPa for IRS and 69 kPa for IGU.

In order to achieve higher resistance in a micropile foundation system installed in sand, the contact surface should be increased (higher length and bigger diameter, or both) instead of changing the micropile reinforcement element.

The micropiles may be installed in isolation or in groups, which can also be classified as a group of micropiles (vertical) or reticulated networks (inclined).

For micropile groups installed in sand, the efficiency coefficient for the shaft resistance was found to be higher than 1.0, while for the tip resistance it was lower than unity according to Francis (1997) and Le Kouby (2003).

The type of loading (monotonic versus cyclic) also influences the micropile behavior. Cyclic loading is the most important type of loading for certain specific structures. Schwarz (2000) observed that, for micropiles with a geometry similar to the one used in this study (5-m long and 130 mm in diameter) installed in sand and pressure grouted, the cyclic loading tends to reduce the bearing capacity when compared with monotonic loads, and it is dependent on the number of cycles and load cycle amplitude, which is in agreement with the works of Chan and Hanna (1980), Turner and Kulhawy (1990), and Briaud and Felio (1986) regarding the cyclic behavior of other types of deep foundations. The tests were conducted with force-controlled cycles of constant amplitude at a given percentage (18 to 55 %) of the tensile capacity. Results showed that more than 10,000 cycles were applied before a sudden drop after a large number of cycles and as a gradual increase in the displacements occurred.

The results on micropiles installed in sand in a pressure chamber showed that about 25,000 cycles were required to achieve micropile failure under cyclic loading with an amplitude of 30 to 45 % of the static failure load (Boulon and Foray, cited by Cyna et al. 2004), while for micropiles installed in medium sand and silt and subjected to reversed loads with increasing amplitude, the capacity estimated by the Davidson method was reduced to as low as 60 % after only two load cycles, as concluded by Cavey et al. (2000), which are in agreement with the ultimate capacity reduction of drilled shafts subjected to two-way cyclic loading observed by Turner and Kulhawy (1990).

The behavior of micropiles and piles installed on different grounds and under different types of loading is well documented. However, the behavior of these elements subjected to cyclic loading has not been exhaustively presented, especially not on the scale and controlled conditions adopted for this study. The main objective of this article is to contribute to a better knowledge of the behavior of micropiles under cyclic loading and to understand its effect on the variation of resistance and monotonic and cyclic stiffness. The proper knowledge of this behavior will allow the use of the obtained results in more realistic ground conditions and loading.

Experimental Layout and Assembly Procedure

A global view of the experimental layout is shown in **Fig. 1**. The micropiles were installed in a cylindrical soil container measuring 2 m in diameter and 3.5 m in height. Because of space constraints related to the available height inside the laboratory, the micropile tip was close (65 cm) to the bottom of the layout (rigid boundary), and the placement of the micropiles into the experimental layout had to be carried out before filling the container with sand, which may have caused a reduction of resistance due to the unstable structure of the sand in the vicinity of the specimens.

Fig. 1 shows the apparatus used to perform the Flat Plate DMT, according to ASTM D6635-01, *Standard Test Method for Performing the Flat Plate Dilatometer*. The DMTs were performed in some layouts to characterize the sand placed in the soil container.

The load was applied to the models using a 200 kN hydraulic actuator with two unidirectional hinges, one on each end, placed orthogonally in order to simulate the behavior of a 3-D hinge and a steel reaction frame.

The micropiles were prepared with nonreturn valves that feature rubber rings that protect the grout exit holes (GEHs; i.e., tube à manchette). The assembly procedure included the placement of the micropiles in the soil container (**Fig. 2**), filling

FIG. 1 Test layout with Dilatometer Test (DMT) equipment.

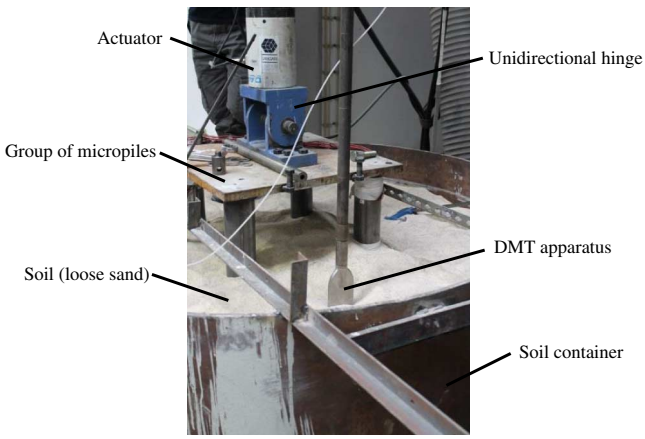

FIG. 2
Micropile positions in layouts – front and top view.

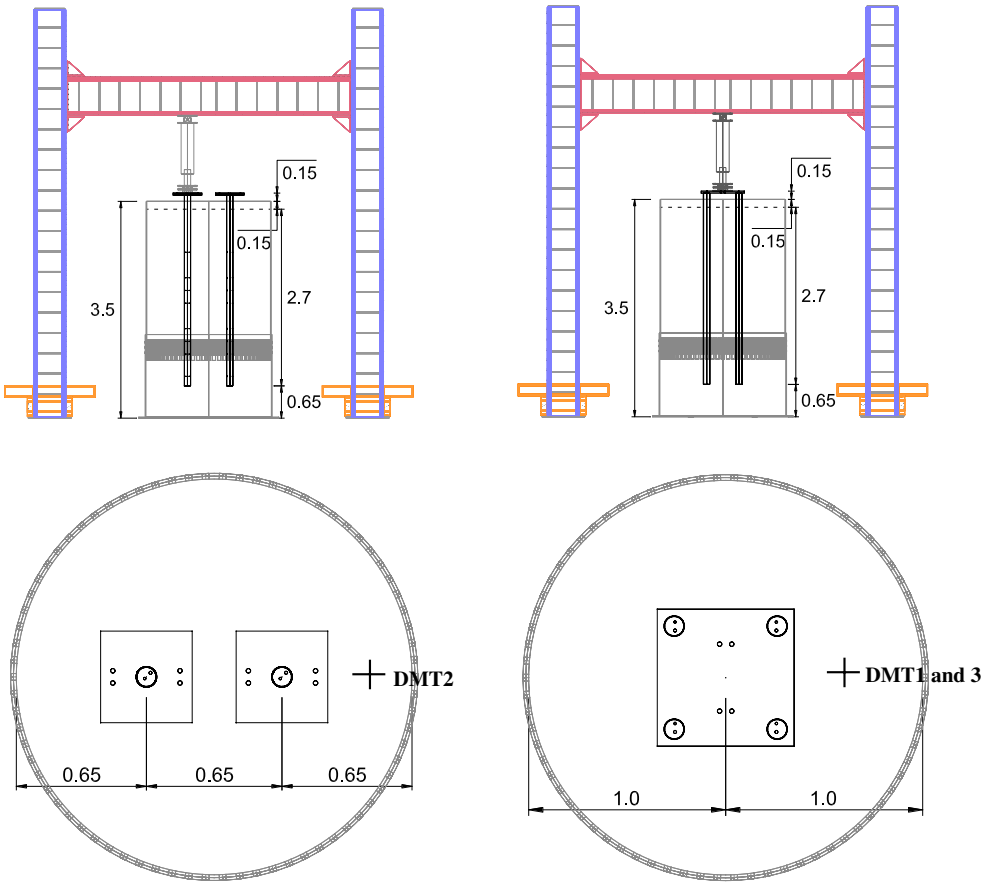

the soil container while controlling the sand's volume and weight, load testing the ungrouted micropiles, grout injection using the prepared pressuring vessel with an injection pressure close to 0.2 MPa, load testing the grouted micropiles (7 days after grout injection), and soil discharging and storage for reuse.

Table 1 presents a summary of the tests performed according to the type of micropile and loading protocol as well as the obtained resistance (R) and monotonic stiffness (k_m) for each case. Both resistance and monotonic stiffness will be discussed later in the paper. The loading sequence was similar for each layout. Ungrouted micropiles were loaded first in compression and then in tension with the aim of evaluating the improvement caused by the grout injection. After the grout was injected, the test proceeded in compression, and followed by tension. In the designations, M stands for single micropile while G stands for group. As the lateral resistance is the highest contributor to the total resistance in this type of foundation, it is expected that the ground conditions after grouting should not differ substantially from what would be found if no prior load testing was performed. The sand was placed in a loose state and the triaxial test results showed no difference between the peak and constant volume friction angle. On the other hand, the micropile surface is very smooth, which leads to low disturbance of the surrounding soil. Finally, it is expected that the grout injection improved the soil around the pile and minimized the changes imposed during prior testing.

The initial stress level of the sand in the layout was lower than typical in situ conditions. The maximum vertical stress of the soil was, on average, 56 kPa for the conditions considered. Although these are not ideal test conditions, which would require full-scale or centrifuge tests, the results are still relevant and may be used to better understand micropile behavior under monotonic and cyclic loading.

In order to compare the behavior of the micropiles under monotonic and cyclic loading, micropiles from Layout 2 (except micropile M4 under grouted conditions) were tested under monotonic conditions and the remaining layouts were submitted to cyclic loading and followed by monotonic loading until the pile failed. The loading protocol was based on prescribed displacements, as shown in **Fig. 3**. The cycles had a period of 800 s

TABLE 1 Experimental tests description, resistance, and monotonic stiffness.

Layout	Micropile	Test	Grout	Loading		R (kN)	k_m (N/mm)
				No. Cycles	Comp./Tens.		
2	M3	1	–	–	Comp.	−4.04	662
		2	–	–	Tens.	2.28	1,053
		3	x	5	Comp.	−17.37	8,333
		4	x	5	Tens.	2.66	7,692
	M4	5	–	–	Comp.	−2.92	114
		6	–	–	Tens.	2.53	1,220
		7	x	–	Comp.	−22.07	885
		8	x	–	Tens.	7.34	1,176
3	M5	9	–	5	Comp.	−5.66	1,724
		10	–	5	Tens.	3.58	2,273
		11	x	5	Comp.	−42.91	14,286
		12	x	5	Tens.	6.02	20,000
	M6	13	–	5	Comp.	−5.82	806
		14	–	5	Tens.	7.68	3,571
		15	x	5	Comp.	−21.87	6,250
		16	x	5	Tens.	2.29	3,448
4	M7	17	–	5	Comp.	−4.73	1,136
		18	–	5	Tens.	5.17	495
		19	x	5	Comp.	−34.63	6,667
		20	x	5	Tens.	11.47	7,692
	M8	21	–	10	Comp.	−6.68	1,667
		22	–	10	Tens.	5.49	1,053
		23	x	10	Comp.	−31.81	9,091
		24	x	10	Tens.	8.99	7,143
5	G1	25	–	5	Comp.	−26.26	11,111
		26	–	5	Tens.	6.67	12,500
		27	x	5	Comp.	−145.96	17,544
		28	x	5	Tens.	14.24	16,129
6	G2	29	–	5	Comp.	−23.91	20,000
		30	–	5	Tens.	6.36	20,000
		31	x	5	Comp.	−145.47	50,000
		32	x	5	Tens.	21.42	12,500
7	G3	33	–	5	Comp.	−26.14	10,000
		34	–	5	Tens.	6.54	7,143
		35	x	5	Comp.	>−177.35[a]	50,000
		36	x	5	Tens.	37.57	50,000

Note: [a]maximum capacity of the actuator reached.

and amplitude of ±1 mm. The period adopted for the cyclic loading was in accordance with the values used by Schwarz (2000), who applied 20-minute cycles and reduced some potential dynamic effects. Five cycles were applied on all but the tests on micropile M8, where ten load cycles were applied to evaluate the effects of the additional cycles on micropile behavior. In the monotonic tests (and after the cyclic loading) the displacement rate was 0.01 mm/s for the compression tests and 0.005 mm/s for the tension tests. The displacement rates considered for the monotonic loading are in accordance with ASTM D1143, *Standard Test Methods for Deep Foundations under Static Axial Compressive Load*, for the compression tests and ASTM D3689, *Standard Test Methods for Deep Foundations under Static Axial Tensile Load*, for the tension tests.

Test Setup

MODEL PROPERTIES

S355 steel circular tubes, which were 3,000-mm long, were used for the piles and had an external diameter of 101.6 mm and a wall thickness of 3.6 mm. Although the slenderness ratio (L/D = 30) is

FIG. 3 Loading protocols: (1) monotonic tension, (2) monotonic compression, (3) cyclic + tension, and (4) cyclic + compression.

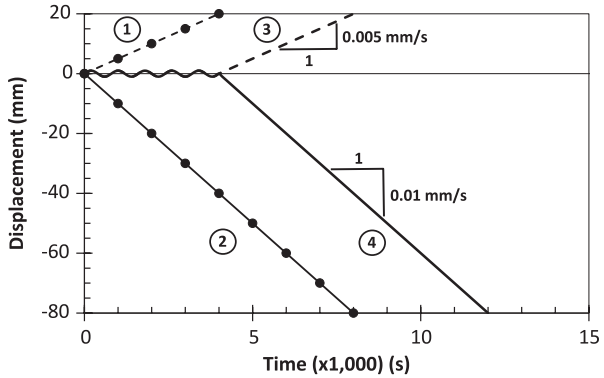

lower than that of typical micropiles, the structural stiffness and resistance is not expected to influence the test results as the geotechnical ultimate load is much smaller than its structural counterpart for the conditions considered in these tests with low density soil. For higher density soils or even higher pressure and better-quality grout conditions, the structural resistance of the micropiles should be accessed as it can drive the design in some cases.

The top plates for the single pile tests (Layouts 2–4) and for the G1 group were square with 450 mm in length/width and 30-mm thick, the G2 group top plate was 600-mm long/wide and 40-mm thick, and the G3 group was assembled with a top plate that was 675-mm long/wide and 30-mm thick. These plates were placed above the ground level.

The GEH positions, number, and diameters changed between each layout in order to obtain a more uniform grout distribution along the micropile wall. The diameter on the lower levels was reduced because there was a higher grout flow on those sections. **Fig. 4** shows the geometry for single and group layouts.

SAND PROPERTIES

The soil used in the tests was a poorly graded sand (SP) according to the unified soil classification system (ASTM D2487, *Standard Practice for Classification of Soils for Engineering Purposes (Unified Soil Classification System)*), and its grain size distribution is presented in **Fig. 5**. Minimum and maximum values for the unit weight were determined according to ASTM D4253-00, *Standard Test Methods for Maximum Index Density and Unit Weight of Soils Using a Vibratory Table*. Specific gravity was determined according to ASTM D854-05, *Standard Test Methods for Specific Gravity of Soil Solids by Water Pycnometer*, and LNEC NP-83, *Soils: Particles Density—Pyknometer Method (in Portuguese)*. The main physical properties obtained for the sand are presented in **Table 2**. For the determination of the soil's mechanical properties, consolidated drained triaxial tests were conducted by considering four different soil densities with three different confining stresses. In terms of friction angle and elasticity modulus, the results obtained are presented in **Table 3**.

FIG. 4
Micropiles geometry: GEH positions.

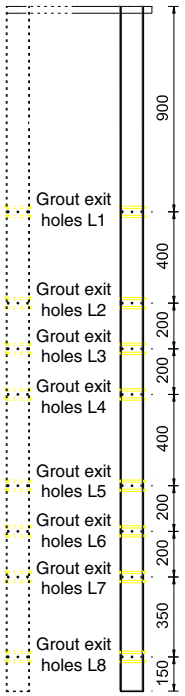

Grout exit holes positions and geometries			
Grout exit holes Level	**Layout 2**	**Layout 3**	**Layout 4-7**
1		6Ø6	
2		6Ø6	6Ø6
3	3Ø8	6Ø8	6Ø6
4		6Ø8	6Ø8
5		6Ø8	6Ø8
6	3Ø8	6Ø8	6Ø8
7		6Ø8	6Ø8
8	3Ø8	6Ø8	6Ø8

FIG. 5 Sieve analysis curves.

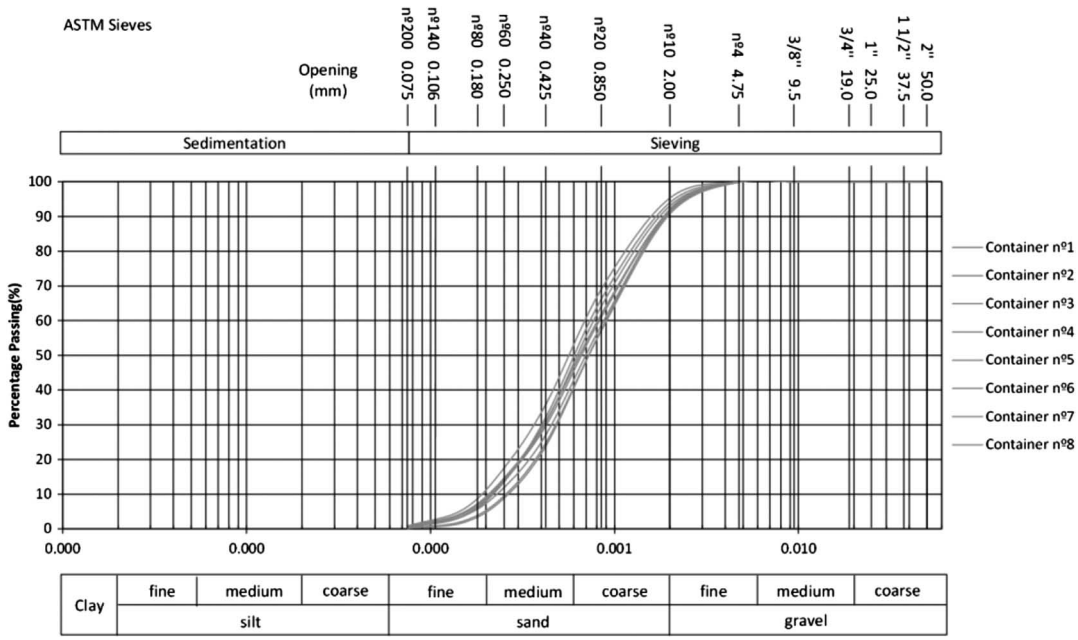

TABLE 2 Soil physical properties.

D_{50} (mm)	C_u	C_c	$\gamma_{d,min}$ (kN/m^3)	$\gamma_{d,max}$ (kN/m^3)	ρ_{min} (gr/cm^3)	ρ_{max} (gr/cm^3)	e_{max}	e_{min}	G_S
0.59	4.43	0.97	14.7	18.9	1.50	1.93	0.76	0.37	2.64

TABLE 3 Friction angle and elasticity modulus (triaxial tests).

ρ (g/cm^3)	Ø' (°)	Confining Stress (kPa)	E_{tan} (MPa)
1.58	33.8	50	10.26
		100	18.83
		200	33.85
1.63	36.3	50	22.58
		100	46.74
		200	56.67
1.73	37.1	50	23.41
		100	51.15
		200	104.33
1.75	44.0	50	37.12
		100	55.02
		200	104.33
1.88	44.7	50	77.70
		100	94.80
		200	158.21

The mean density index (I_D) of the sand was determined for each layout with an associated error of ±3 % (average of 31.8 % for the six layouts considered) as well as the unit weight with an average value of 16 kN/m^3.

The DMT1 and DMT2 tests were performed on Layouts 7 and 4, respectively, both after the grout injection. The DMT3 test was performed on Layout 5 after the ungrouted tests on the G1 group and before grouting took place.

From what was observed during the tests and by the analysis of the results, it is possible to state that the sand properties improved after the grouting process. Test DMT3 was performed before grouting and presented lower readings (of the contact pressure, p_0, and the expansion pressure, p_1) and soil parameters than DMT1 and 2.

The DMTs carried out on layouts with grouted micropiles yielded readings along the entire height because the confining horizontal stress was high enough to pressurize the DMT blade membrane. At some soil depths and in the test in the layouts with ungrouted micropiles (DM3), that did not happen, as shown in **Fig. 6**.

GROUT PROPERTIES

The following mix proportions were adopted for the grout, which are similar to the composition used by Veludo et al. (2012) and are a typical composition used by the industry: water/cement ratio 0.4, with type II: 32.5 N portland cement, 1 % of modified

FIG. 6 DMT results: (a) corrected readings, p_0 (kPa); (b) corrected readings, p_1 (kPa); (c) horizontal stress index, K_d.

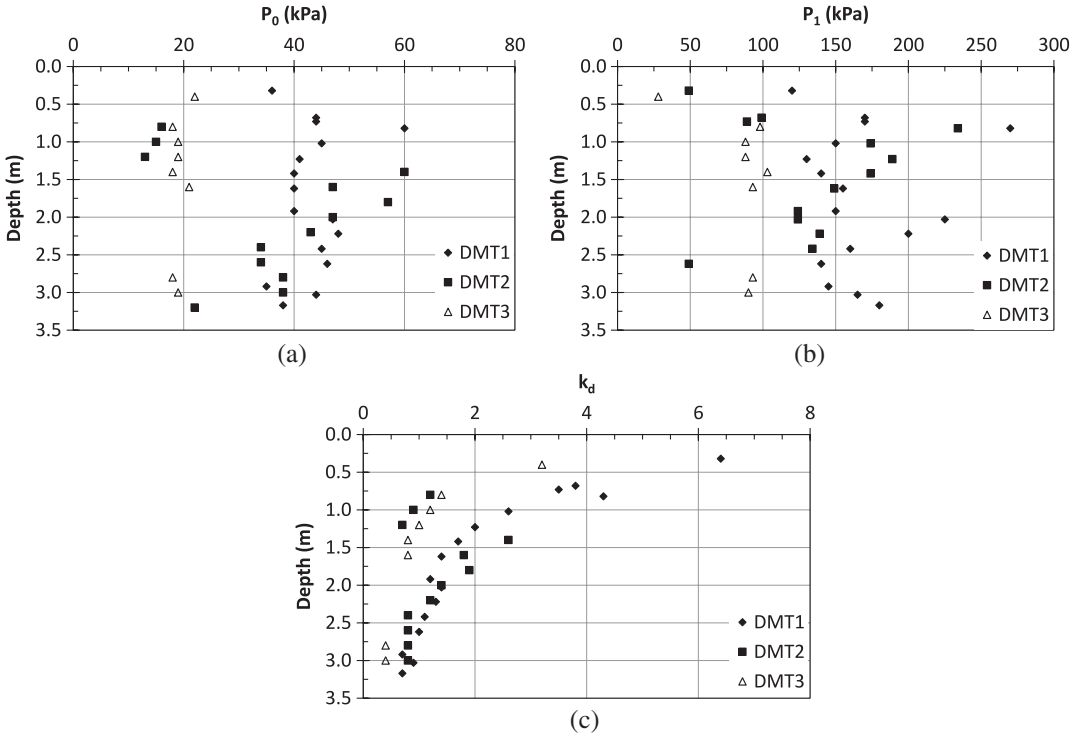

polycarboxylate admixture (high-range water reducer); and 1 % expansive admixture.

Tests were carried out to control some properties of the grout, such as fluidity, exudation, volume variation, and compressive strength. **Fig. 7** displays the results obtained on the fluidity tests in each layout, as well as the limit defined by the appropriate standard (CEN EN 447, *Grout for Prestressing Tendons – Basic Requirements*) and only 2 of the 54 tests (one on M5 and another on one G3 micropile) presented results higher than 25 s (28 and 26 s, respectively).

The results of the exudation test (CEN EN 445, *Grout for Prestressing Tendons – Test Methods*) on the grout of Layout 3 were unsatisfactory for M5 (3.7 %) and satisfactory for M6 (1.3 %). For Layout 4, the results were both satisfactory for M7 and M8 (1.7 and 1.3 %, respectively), and for Layout 5, the result was unsatisfactory with 3.3 % on the three mixtures measured.

FIG. 7 Grout fluidity test results.

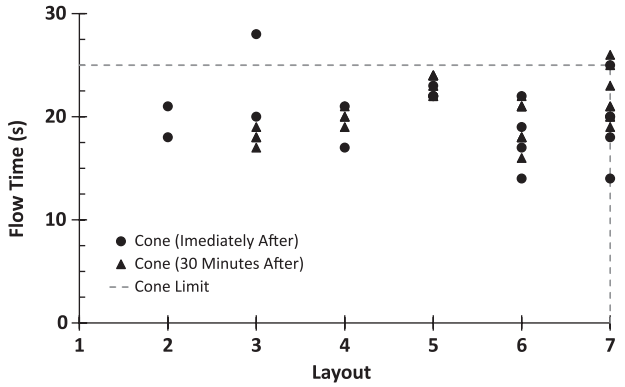

The volume variation was controlled according to CEN EN 445, and the results obtained for Layout 4 were high according to the limits (−3.4 and −5.4 %) but were satisfactory for Layout 5 (0 % for the four mixtures tested).

Some of the problems observed with the exudation and volume variation results are due to the low rotation speed of the available electrical mixer. It should be higher in order to achieve better-mixed grout components.

Finally, the compressive strength was determined, according to CEN EN 447 and CEN EN 196-1, *Methods of Testing Cement – Part 1: Determination of Strength*, for all the layouts assembled, both for 7 and 28 days after mixture and injection. The results obtained were all satisfactory according to the limits imposed by the standard (27 and 30 MPa, respectively, for 7 and 28 days), apart from the results of Layout 6 (22.3 and 24.1 MPa for 28 days) and in one mixture of Layout 7 (22 MPa for 28 days) because of excessive exudation of the water that created a soft layer on top of the specimen, reducing the effective resistant cross section.

After the load tests were concluded on each layout, the sand was removed, the micropiles were exhumed, and the grout distribution was measured and recorded. There was some scatter in the distribution of the grout from test to test, which is supposed

to be similar to what occurs in the real production of micropiles. It was not possible to reproduce the same grout geometries in two different micropiles and consequently reproduce the same resistant properties. **Fig. 8** shows examples of the grout distributions obtained.

It was observed that the grout did not come out of the tube uniformly. Because the sand was very loose, and the vertical effective stress was low, the grout spread more horizontally than vertically, as preferable, along the tube walls. This is the reason why the grout was connected to the tube walls only close to the GEHs region and not along the full length of the micropile. In **Fig. 8a**, it is possible to observe a horizontal grout plate that formed between the two single micropiles.

Table 4 shows the results both in terms of the medium diameter obtained for the grouted areas as well as the total grouted length and the percentage of the grouted length related to the embedded length.

Experimental Results

OVERVIEW

The results presented in this section are the force-displacement curves for each test, the monotonic resistance (or after cycles, when applicable), and the stiffness both of the cyclic and the initial/postcyclic branches.

The test sequence was kept unchanged in all layouts prepared. All models were tested first without grout in compression (monotonic or cyclic + monotonic) and after in tension (monotonic or cyclic + monotonic). After that sequence, the pressured grout was applied, and then compression tests with grouted models (monotonic or cyclic + monotonic) were carried out, which were followed by tension tests (monotonic or cyclic + monotonic).

To allow a comparison of results for the same structural performance, it was defined a failure displacement of 10 % of the micropile diameter (10.16 mm) for tension tests and 20 % (20.32 mm) for compression tests. The value of 10 % of the diameter is commonly accepted for design purposes, and for the tension tests, it can be seen that the resistance is fully mobilized for a much smaller displacement. However, analyzing the shape of the force-displacement curves of the compression tests, it was observed that the failure load occurs for higher displacements because of the influence of the end bearing. For this reason, a failure displacement of 20 % of the micropile diameter (around 20 mm) was adopted. This value would yield a settlement under service conditions that would be acceptable for most geotechnical constructions, including foundations for wind turbines.

RESISTANCE

Figs. 9 and **10** present, respectively, the global and an example of the cyclic portion of the force-displacement curves obtained for the grouted and ungrouted compression tests. Similarly, **Figs. 11**

FIG. 8

Grout distribution: (a) single tests (horizontal plate) – Layout 2; (b) single tests – Layout 4; and (c) group tests – Layout 6.

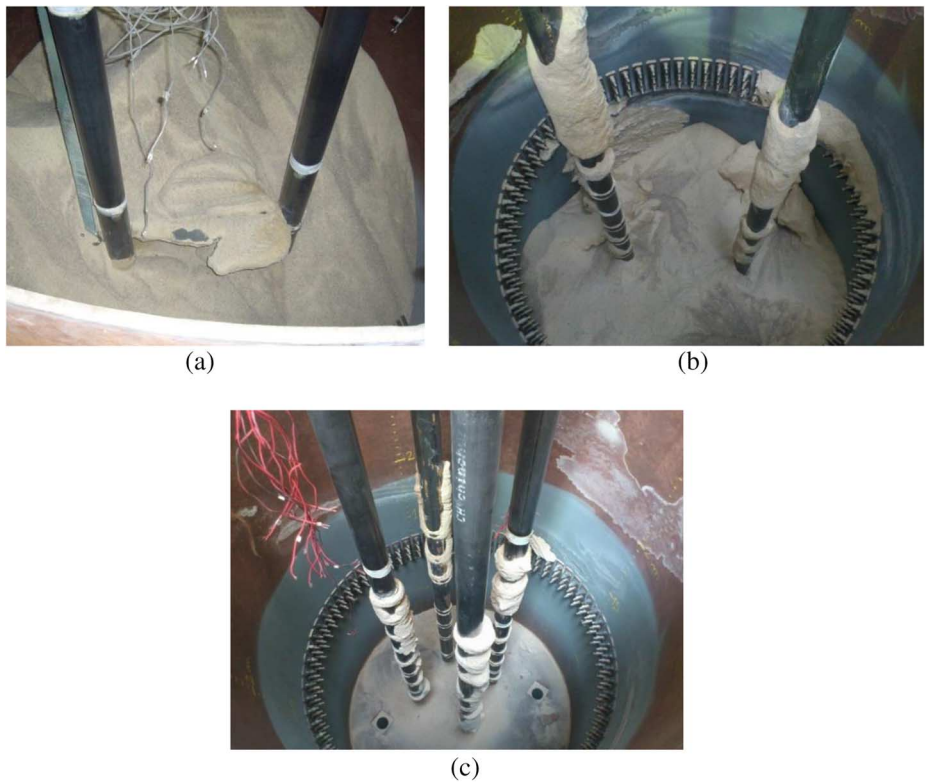

TABLE 4 Grout geometry and unit shaft resistance.

Layout	Micropile	Grout	Medium Diameter (mm)	Embedded Length (mm)	Grouted Length (mm)	Grouted Length (%)	q_s (kPa)
2	M3	No	101.6	2,700[a]	0	0	2.6
		Yes	156.0[a]	2,700[a]	0[b]	0[b]	3.0[c]
	M4	No	101.6	2,700[a]	0	0	2.9
		Yes	156.0[a]	2,700[a]	945[a]	35[a]	11.7[c]
3	M5	No	101.6	2,740	0	0	4.0
		Yes	163.0	2,740	1,010	37	7.0[c]
	M6	No	101.6	2,700[a]	0	0	–
		Yes	156.0[a]	2,700[a]	945[a]	35[a]	–
4	M7	No	101.6	2,670	0	0	6.0
		Yes	158.0	2,670	1,010	38	15.9[c]
	M8	No	101.6	2,700	0	0	6.3
		Yes	146.0	2,700	850	31	12.9[c]
5	G1	No	101.6	2,690	0	0	1.9
		Yes	140.0	2,690	725	27	7.1[c]
6	G2	No	101.6	2,690	0	0	1.8
		Yes	147.0	2,690	1,123	42	8.5[c]
7	G3	No	101.6	2,700	0	0	1.9
		Yes	142.0	2,700	960	36	19.3[c]

Note: [a]value not measured; mean value from M5, M7, and M8 micropiles.

[b]assumed value because of the low grout distribution along the outside pile wall.

[c]mean unit shaft resistance on the grouted length. The mean unit shaft resistance on the ungrouted length of the micropile is similar to the value of the ungrouted micropiles.

FIG. 9 Force-displacement curves (single tests, compression): (a) ungrouted tests and (b) grouted tests.

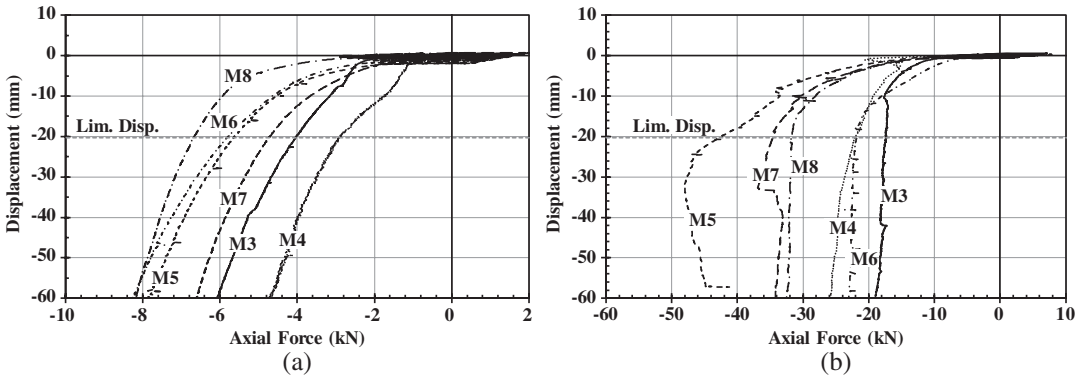

FIG. 10 Detail of cyclic tests on M5 – compression: (a) ungrouted test and (b) grouted test.

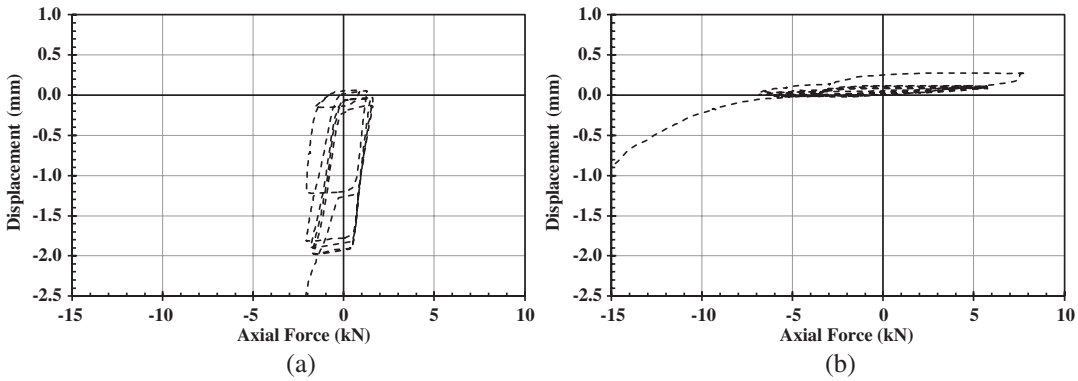

FIG. 11 Force-displacement curves (single tests, tension): (a) ungrouted tests and (b) grouted tests.

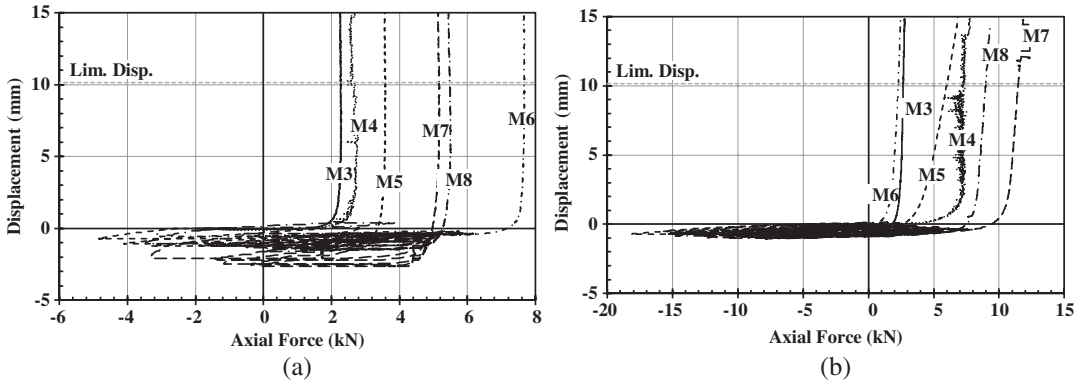

FIG. 12 Detail of cyclic tests on M7 – tension: (a) ungrouted test and (b) grouted test.

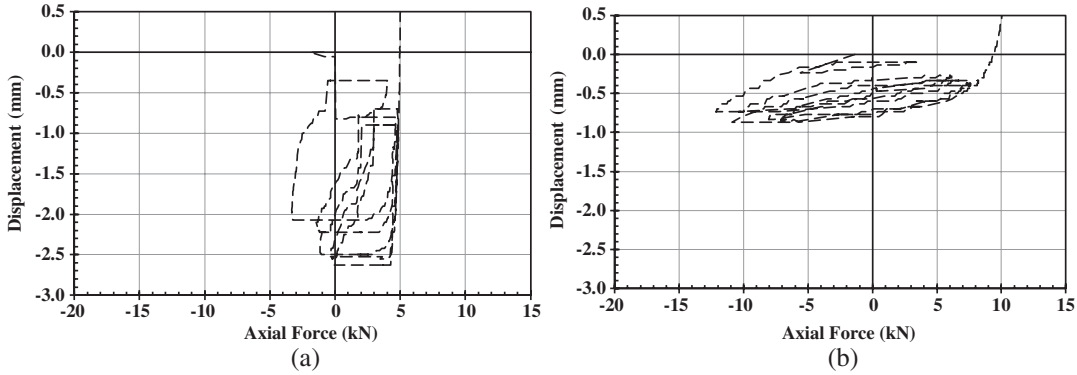

and 12, respectively, show the global and an example of the cyclic portion of the force-displacement curves of the tension tests. It may be clearly observed that the load amplitude during the cyclic phase of the loading was larger for the grouted micropiles, which shows the benefit and the improvement caused by the grout injection.

The global and the example of the cyclic portion of the force-displacement curves of the compression tests on group micropiles are presented in Figs. 13 and 14, respectively, while the global force-displacement curve and an example of its cyclic portion of the tension group tests are presented in Figs. 15 and 16. The beneficial effects of grouting may be observed, as the load

FIG. 13 Force-displacement curves (group tests – compression): (a) ungrouted tests and (b) grouted tests.

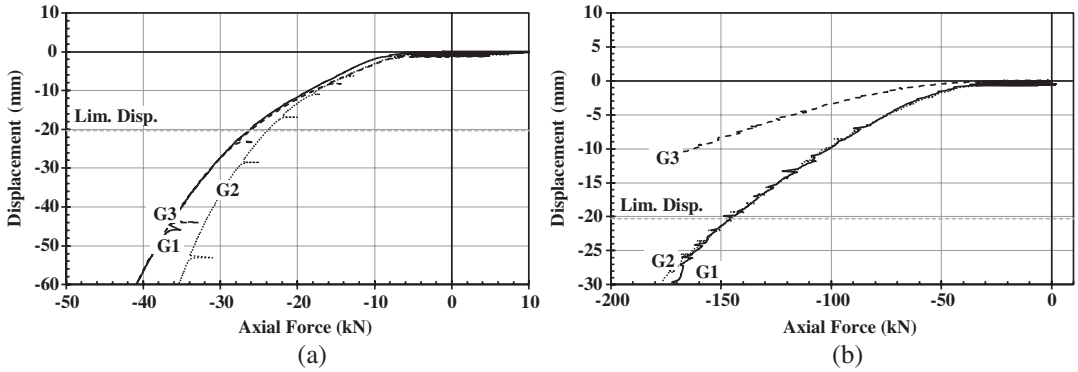

FIG. 14 Detail of cyclic tests on G1 group – compression: (a) ungrouted test and (b) grouted test.

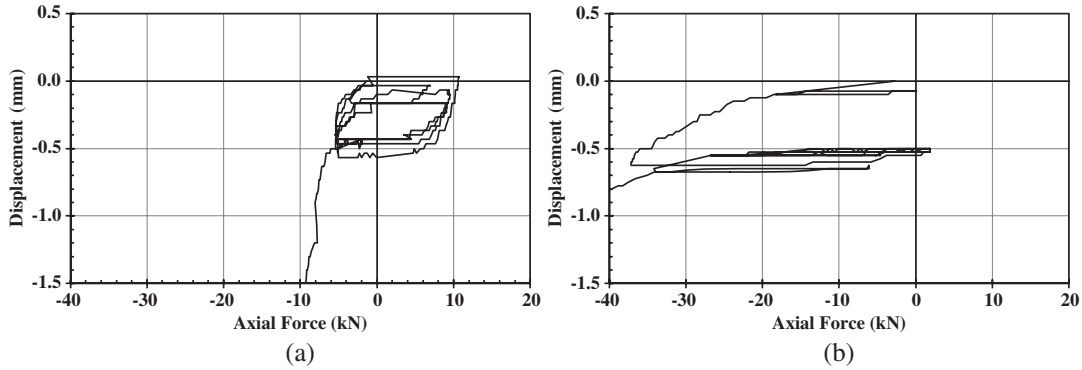

FIG. 15 Force-displacement curves (group tests – tension): (a) ungrouted tests and (b) grouted tests.

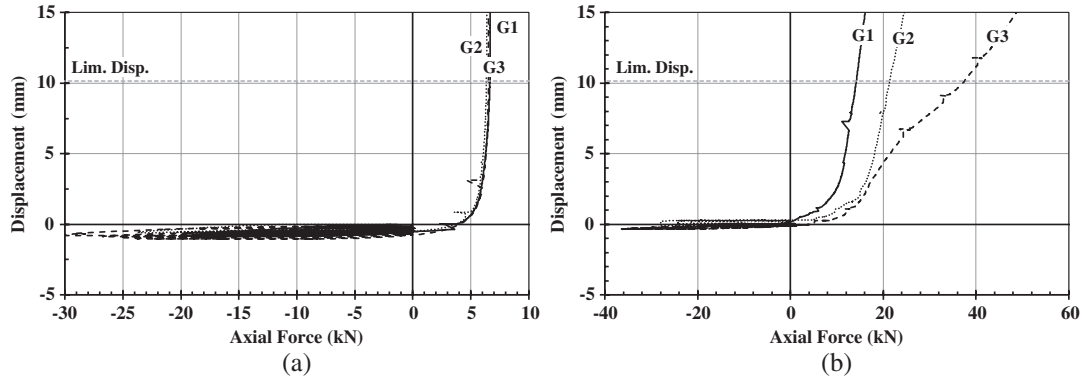

FIG. 16 Detail of cyclic tests on G3 group – tension: (a) ungrouted test and (b) grouted test.

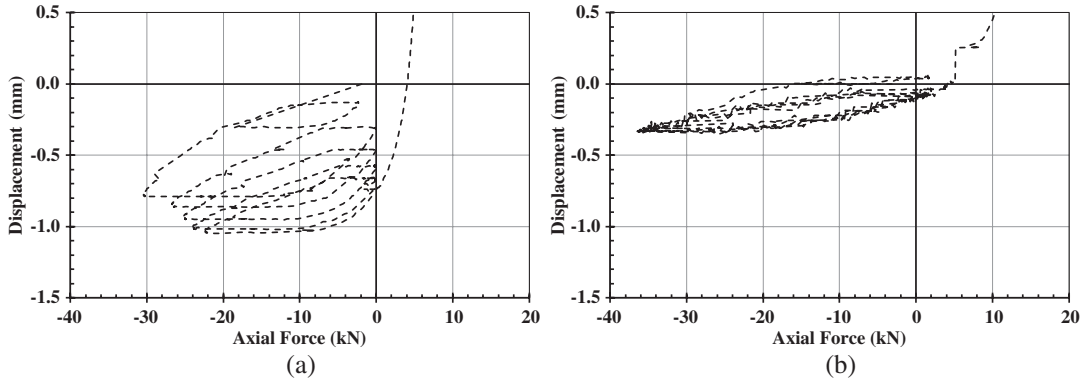

amplitude during the cycles is, once again, higher for the grouted micropiles.

The results obtained, in terms of resistance and static (or postcyclic when applicable) stiffness are presented in **Table 1**, for single and group tests. The resistance corresponds to the force obtained for the limit displacement considered for each test according to **Figs. 9**, **11**, **13**, and **15**.

The comparison between the grouted and ungrouted micropiles is presented in **Table 1** and shows a substantial improvement on the resistance between 280 and 660 % for compression tests on single micropiles. For the tension tests, the improvement varies between 20 and 190 % of the resistance obtained with the ungrouted tests (excluding micropile M6, where both the tensile resistances, ungrouted and grouted, were different than expected because the ungrouted value was much higher and the grouted value is much lower than the mean values of the remaining tests). The gain in resistance was as expected and was due to the following: the increase of unit shaft resistance, the micropile diameter,

the improvement of the soil characteristics as it was observed in the DMT tests, and improvement of the unstable poured sand in the vicinity of the micropiles.

In the case of the group tests, the improvement of the resistance caused by grouting varies between 460 and 580 % for compression tests while, for tension tests, the improvement varies between 110 and 470 %.

Apart from the M7 single micropile, whose compressive resistance was lower than expected, and M6 whose tensile resistance was higher than expected, the compressive resistance was always higher, as expected, than the corresponding tensile resistance. For ungrouted single tests, the compressive resistances were 20 to 80 % higher than the tensile resistances. For the grouted cases, that difference varied from 200 to 850 % of the tensile resistance. It should be stated that for settlements measuring more than 20 mm, the compressive resistances of the ungrouted tests on M6 and M7 were greater than the values obtained for the tension tests. This difference is also influenced by the proximity to the rigid boundary of the layout, which will increase the tip effect and will lead to an increase in the compressive resistance.

For the group tests, the compressive resistance was 280 to 300 % higher than the tensile resistance for ungrouted micropiles, while for grouted micropiles it varied from 370 to 900 %.

It was also found that for the conditions of the ungrouted tests, the group spacing effect was not significant. If the results for the G1 group (spacing of 3B) are used as a reference, in compression, a reduction of 9 % at 4B and a 0 % reduction for 5B spacing was calculated. In tension, a reduction of 5 % was calculated for 4B spacing and 2 % for 5B spacing, which agrees with Sabatini et al. (2005).

In the grouted tests, the results of the resistant values of each micropile show a broader variation, but in these cases, they are mainly due to the grout distribution along the pile length. In the compression tests, similar results were found for the 3B and 4B groups. For the 5B group, the equipment capacity was reached before the 20-mm limit displacement was measured. The load-displacement curve in **Fig. 13** shows that the behavior of group 5B is stiffer than that of the 3B and 4B tests. For a 10-mm displacement, a resistance increase of 61 % was found for group 5B. In the tension tests, an increase of 50 % in 4B and 164 % in 5B was observed.

The group effect was observed by the comparison between the single and the corresponding group results. The mean value of resistance for the single compression ungrouted tests was $\overline{R}_{c;single} =$ 5 kN, while the corresponding mean value for the group was $\overline{R}_{c;group} = 25$ kN, which resulted in an efficiency of $\eta = 125$ %. For the tensile ungrouted cases, the single pile mean resistance was $\overline{R}_{t;single} = 3.8$ kN, while the group yielded $\overline{R}_{t;group} = 6.5$ kN, and the efficiency was only $\eta = 43$ %. If the results from the tests without cyclic loading prior to the monotonic loading (M3 and M4) and M7 are excluded, because of the unreasonable result, the mean value for the resistance for the single compression ungrouted tests was $\overline{R}_{c;single} = 6.0$ kN, which corresponds to an efficiency of $\eta = 104$ %, closer to $\eta = 100$ %, which is expected for this situation.

The grouted tests under compression yielded $\overline{R}_{c;single} =$ 28.5 kN for the single micropiles and $\overline{R}_{c;group} = 145$ kN for the groups G1 and G2 ($\eta = 127$ %). The mean tensile resistance obtained for the single grouted tests was 7.3 kN while for groups it was 24.4 kN ($\eta = 84$ %).

Taking into account the comparison between the compressive and the respective tensile resistance, it may be observed that for the ungrouted micropiles, the ratio $R_{t;single}/R_{c;single}$ varies between 0.6 and 0.9 (excluding micropiles M6 and M7 because of the reasons presented previously) and between 0.1 and 0.3 for grouted models of single micropiles. The bigger differences between the tensile and the compressive grouted resistances are related to the fact that the tensile force is applied after the compressive force, which can lead to a detachment of some of the grout during compression, thereby reducing the tensile resistance.

For the groups, values of $R_{t;group}/R_{c;group}$ close to 0.3 were obtained for ungrouted micropiles and of 0.1 to 0.2 for the grouted micropiles.

The obtained resistances are related to some singularities on the micropile geometry. In the case of the ungrouted single micropiles, it was observed that for Layout 2 the resistances were lower than the other two single layouts with ungrouted micropiles because of the lower number of GEH levels. Those levels and respective protections added extra side resistance to the micropiles. In terms of grouted micropiles, it was observed that the amount of grout measured around the tube at the end of the tests is related to the resistance obtained. The M5 micropile was clearly the micropile that had more grout around the pile and, consequently, provided more resistance than the others. In the case of micropile M3, a horizontal grout plate was created, which provided high compressive resistance; however, it broke close to the end of the test and the subsequent tensile resistance was low. The M4 micropile presented more grout than the others close to the tip of the tube, which improved both the compressive and the tensile resistance.

The grout distribution on the groups also influenced their resistance. On G1 the compressive resistance was high because one horizontal grout plate formed in the middle of the micropiles of this group, connecting some of them, but which broke after the test, leading to a relatively low tensile resistance. The G2 group had more grout around the piles, which improved both the compressive and the tensile resistances. G3 had a grout layer connected to the soil container that substantially improved the compressive and tensile resistances but is clearly not representative.

In **Table 4**, the percentage of grouted length in comparison with the embedded length, the corresponding medium diameter of the grout, and the mean unit shaft resistance (q_s) for the

FIG. 17 Cyclic and monotonic stiffness estimation procedure.

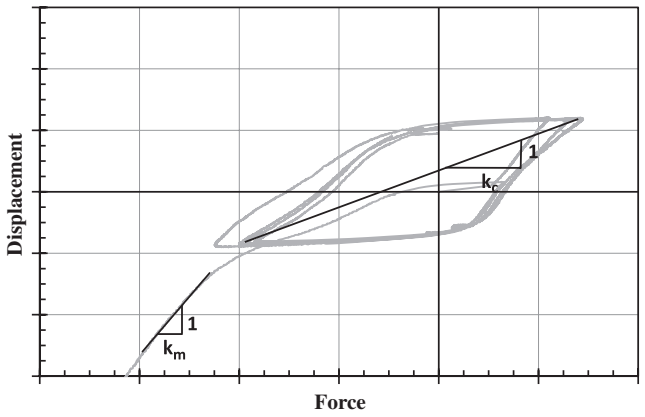

tension tests is shown. Because the grouted length is always smaller than the embedded length for grouted micropiles, it was assumed that the mobilization of a value of q_s in the ungrouted length as determined on the previous ungrouted tests while in the remaining length (grouted length) a higher value of q_s was obtained was a characteristic of the grouted length.

The mean unit shaft resistance ranged from 2.6 to 6.3 kPa for the single ungrouted micropiles and from 3.0 to 15.9 kPa for the grouted single micropiles. For these soil properties, considering a medium density of 1.58 g/cm^3, a friction angle of 33.8°, and a friction angle between the soil and the ungrouted pile of 20°, the resulting mean unit shaft resistance is 3.8 kPa. For the grouted micropiles, a value of 7.0 kPa was obtained while considering the same soil properties but with a friction angle of 33.8° between the soil and the grouted pile. Both of the unit shaft resistances

FIG. 18 Single tests' cyclic stiffness: (a) M3, (b) M5, (c) M6, (d) M7, and (e) M8.

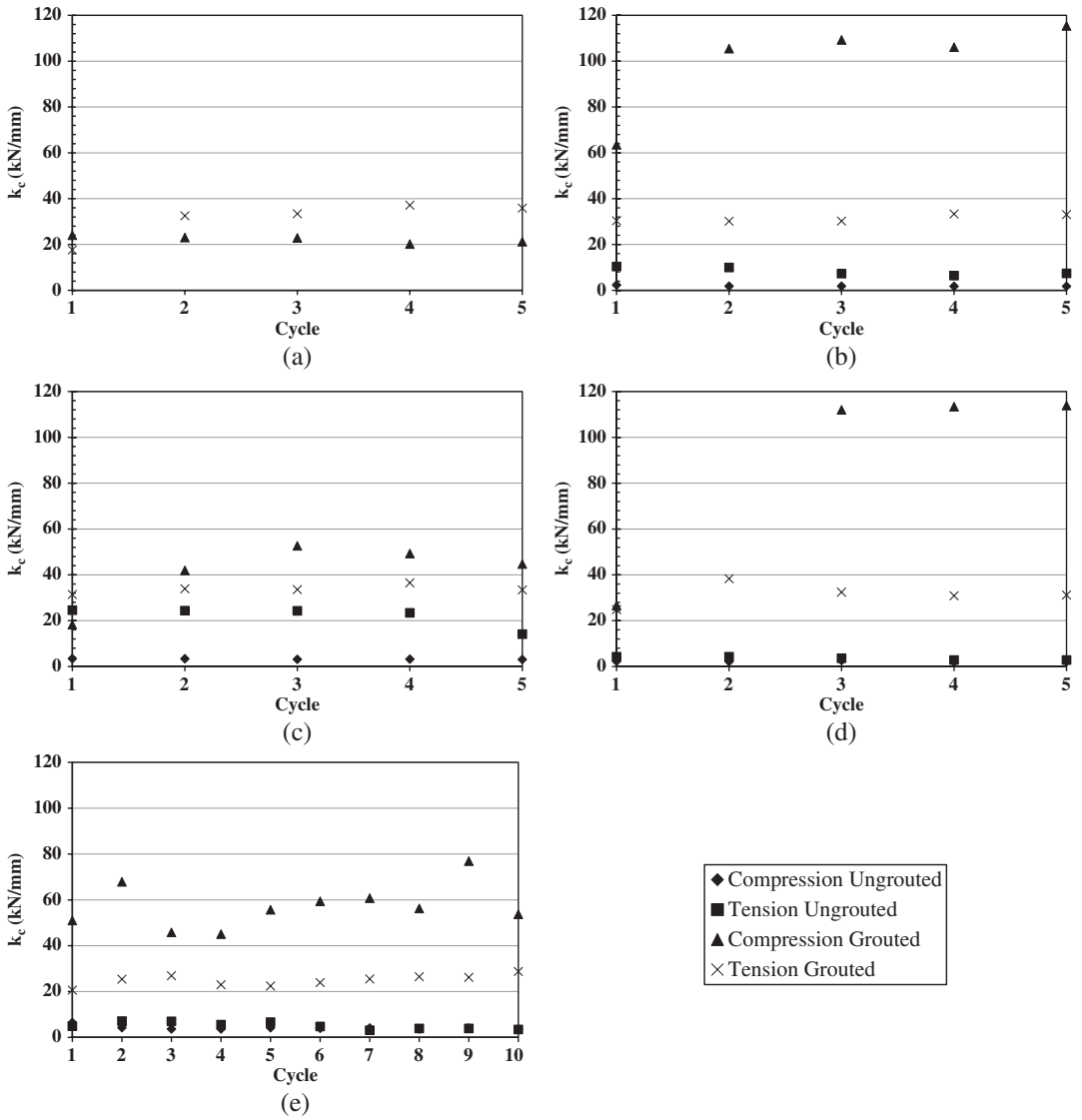

estimated for grouted and ungrouted tests are within the range of values obtained in the experimental tests.

Similarly, the unit shaft resistance varied between 1.8 and 1.9 kPa for ungrouted group micropiles and between 7.1 and 19.3 kPa for the grouted group cases.

Table 4 shows that the unit shaft resistance of the piles in the groups is lower than the single micropiles, and that is the reason why the group efficiency in tension is lower than 100 %. The explanation to this finding concerns the pile installation procedure. As the groups were placed before the sand was poured, the ability to spread the sand on the central area between the piles was limited, and so it was likely the sand had a looser state, resulting in lower friction angles and, consequently, lower values of unit shaft resistance.

STIFFNESS

Regarding the initial monotonic stiffness (k_m) measured after the cyclic phase, as shown in **Fig. 17**, it was observed that the values obtained were higher for grouted than for ungrouted tests, both for single and for group micropiles, as expected and as shown in **Table 1**. The effect of the grouting on the stiffness of the single micropiles (k_{m_gr}/k_{m_ung}) led to a variation between 1.0 and 15.4 times the stiffness of the ungrouted piles. For the group tests, the same variation was between 1.3 and 7.0 (excluding G2 where the tensile grouted stiffness was lower than the corresponding ungrouted test). The improvement caused by the grout is more prominent on the single micropiles than in the groups, which should be related with the higher average grouted diameter registered in the single micropiles in comparison with the groups of micropiles.

It was found that the mean value of the monotonic stiffness of the single micropiles without cyclic loading was lower than for the micropiles with cyclic loading. The values obtained for the ratio of stiffness's were in the range of 0.1 to 0.6. However, it is important to note that the micropiles without cyclic loading were the micropiles from Layout 2 (M3 and M4), which had fewer GEH levels and, consequently, lower resistance and stiffness than the rest of the micropiles.

The cyclic stiffness (k_c) was determined using the method presented in **Fig. 17**. In this generic representation of cyclic loading, the cyclic stiffness is defined as the inverse of the slope of the line connecting the two cycle extremes.

The values obtained for each test where the cyclic loading was applied are presented in **Fig. 18** for the single tests and in **Fig. 19** for the group tests.

The cyclic tensile stiffness was higher than the value obtained in the compression test. This is likely to be caused by an increase in the sand density after the ungrouted compression tests, resulting in higher ungrouted tensile cyclic stiffness, while in the grouted cases it may occur because of the detachment of some of the grout after the compression grouted tests, leading to lower values for tensile-grouted cyclic stiffness.

FIG. 19 Group tests' cyclic stiffness: (a) G1, (b) G2, and (c) G3.

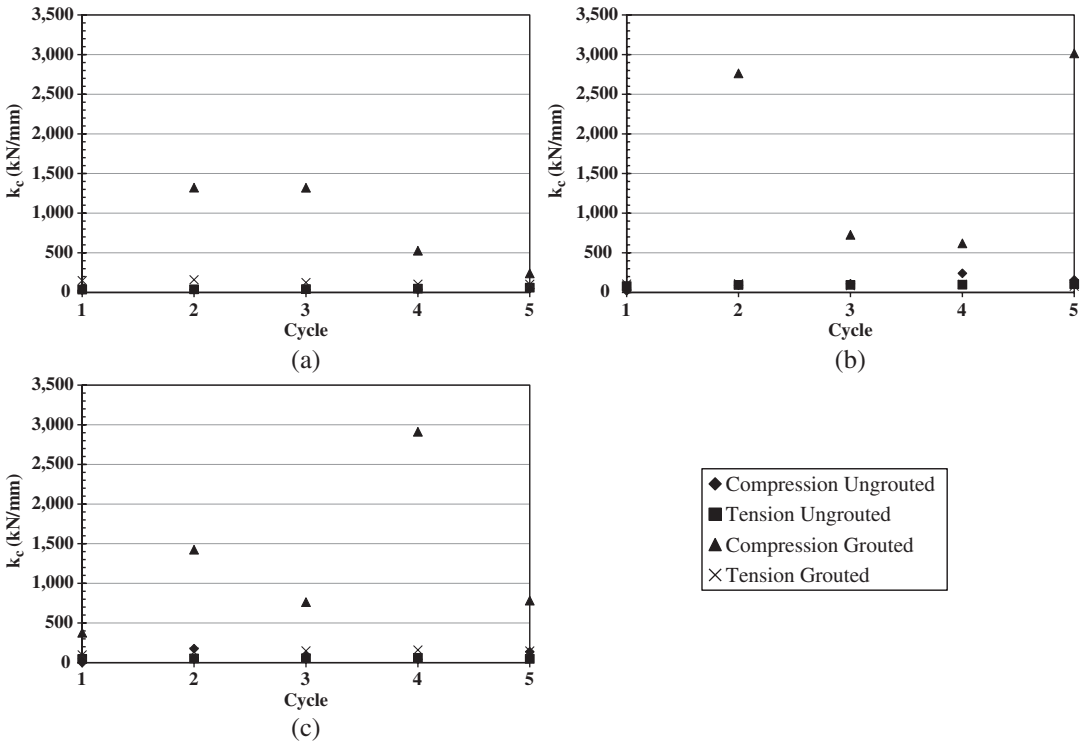

From the analysis of **Figs. 18** and **19**, it is possible to observe that the grouted micropiles presented a higher cyclic stiffness than the corresponding ungrouted micropiles, both for single and group tests. This was as expected and in the same manner as in the static/postcyclic stiffness. For this analysis, the mean value for the stiffness of the five cycles (or ten cycles in the case of the M8 micropile) was considered.

It was observed, in **Figs. 18** and **19**, that the cyclic stiffness variation from cycle to cycle is very small, even in the case of M8 micropiles where a higher number of cycles (ten cycles instead of five cycles, as in the other micropiles) was applied.

Conclusions

The experimental tests in small-scale micropiles can be a viable tool for the calibration of a numerical model for the estimation of the behavior of micropiles installed in soils with different properties.

In both the single and the group tests, grouting improved the micropiles' resistances, as larger cycles (higher force amplitudes) were required to mobilize an imposed displacement in grouted micropiles.

In the vast majority of the tests, except for M6 and M7, the compressive resistances were higher than the corresponding tensile resistances because of the influence of the end bearing. For both single and group tests, the differences were higher for grouted than for ungrouted micropiles. For higher displacements of M6 and M7, higher compressive than tensile resistances were obtained, which agreed with the rest of the tests.

The micropile spacing did not significantly affect the results for the ungrouted tests.

A comparison between the mean values of resistance of the single micropiles and the corresponding group micropiles (group effect) showed that the efficiency coefficient was higher than 100 % for the compression tests in the case of the ungrouted tests. If the results from the micropiles without cyclic loading, prior the monotonic, were neglected, the efficiency coefficient was close to 100 %.

The values obtained for the mean unit shaft resistance on single micropiles, both grouted and ungrouted, fell within the analytical estimations made ahead of the tests. The values for the unit shaft resistance for the singles were, on average, 132 % higher for ungrouted tests and 29 % higher for grouted tests when compared with the group micropiles.

The initial monotonic stiffness (or postcyclic when applicable) was, on average, 490 % higher for the grouted than for the ungrouted micropiles. The improvement of the grout was more relevant on the single micropiles where an average improvement of 630 % was obtained compared to an improvement of 200 % for the group cases.

The monotonic stiffness of the micropiles with cyclic loading was, on average, 476 % higher than that obtained for the micropiles without cyclic loading.

In the case of the cyclic stiffness it was concluded that, for every case studied, the grouted micropiles provided higher stiffness than the corresponding ungrouted micropiles, both for compressive and tensile loadings, with an average improvement of 1,280 %. The improvement was much more evident for compression tests than tension tests, and average values of 1,820 and 270 %, respectively, were calculated.

The comparison between the compressive and tensile cyclic stiffness showed that, for the ungrouted single tests, the tensile cyclic stiffness was, on average, 250 % higher than the respective compressive stiffness, while for the grouted tests, an average improvement of 150 % was observed between the compression and tension tests.

For the group tests, and with the exception of the G1 group, the compressive stiffness was, on average, 570 % higher both for ungrouted and grouted tests.

The relevance of the grouting for both strength and stiffness of the micropiles shows how important it is to achieve the best grouting procedure in order to optimize the use of the micropile and promote the highest unit shaft resistance.

ACKNOWLEDGMENTS

This study was undertaken within the HISTWIN2 project and was partially funded by the Research Fund for Coal and Steel (RFS-CT-2010-00031).

The authors would like to thank the FCT (Fundação para a Ciência e Tecnologia) for the grant conceded for the development of the work and to Sika for providing the adjuvants required for the grout production.

References

Alnuaim, A. M., El Naggar, M. H., and El Naggar, H., 2015a, "The Performance of Micropiled Raft in Clay Subjected to Vertical Concentrated Load: Centrifuge Modeling," *Can. Geotech. J.*, Vol. 52, No. 12, pp. 2017–2029, https://doi.org/10.1139/cgj-2014-0448

Alnuaim, A. M., El Naggar, H., and El Naggar, M. H., 2015b, "The Performance of Micropiled Raft in Sand Subjected to Vertical Concentrated Load: Centrifuge Modeling," *Can. Geotech. J.*, Vol. 52, No. 1, pp. 33–45, https://doi.org/10.1139/cgj-2014-0001

Alnuaim, A. M., El Naggar, M. H., and El Naggar, H., 2016, "Numerical Investigation of the Performance of Micropiled Rafts in Sand," *Comput. Geotech.*, Vol. 77, pp. 91–105, https://doi.org/10.1016/j.compgeo.2016.04.002

ASTM D1143, 2013, *Standard Test Methods for Deep Foundations under Static Axial Compressive Load*, ASTM International, West Conshohocken, PA, www.astm.org

ASTM D2487, 2011, *Standard Practice for Classification of Soils for Engineering Purposes (Unified Soil Classification System)*, ASTM International, West Conshohocken, PA, www.astm.org

ASTM D3689, 2013, *Standard Test Methods for Deep Foundations under Static Axial Tensile Load*, ASTM International, West Conshohocken, PA, www.astm.org

ASTM D4253-00, 2000, *Standard Test Method for Maximum Index Density and Unit Weight of Soils Using a Vibratory Table*, ASTM International, West Conshohocken, PA, www.astm.org

ASTM D6635-01, 2007, *Standard Test Method for Performing the Flat Plate Dilatometer*, ASTM International, West Conshohocken, PA, www.astm.org

ASTM D854-05, 2005, *Standard Test Methods for Specific Gravity of Soil Solids by Water Pycnometer*, ASTM International, West Conshohocken, PA, www.astm.org

Briaud, J. and Felio, G., 1986, "Cyclic Axial Loads on Piles: Analysis of Existing Data," *Can. Geotech. J.*, Vol. 23, No. 3, pp. 362–371, https://doi.org/10.1139/t86-051

Bustamante, M. and Doix, B., 1985, "Une Méthode pour le Calcul des Tirants et des Micropieux Injectés (in French)," *Bull. Liaison Lab. Ponts Chaussées*, Vol. 140, pp. 75–95.

Cavey, J., Lambert, D., Miller, S., and Krhounek, R., 2000, "Observations of Minipile under Cyclic Loading Conditions," *Proc. Inst. Civ. Eng. Ground Improv.*, Vol. 4, No. 1, pp. 23–29.

Chan, S. and Hanna, T., 1980, "Repeated Loading on Single Piles in Sand," *J. Geotech. Eng. Div.*, Vol. 6, No. 2, pp. 171–187.

CEN EN 445, 2000, *Grout for Prestressing Tendons - Test methods* (in Portuguese), Comité Européen de Normalisation, Brussels, Belgium, https://www.cen.eu

CEN EN 447, 2000, *Grout for Prestressing Tendons - Basic Requirements* (in Portuguese), Comité Européen de Normalisation, Brussels, Belgium, https://www.cen.eu

CEN EN 196-1, 2006, *Methods of Testing Cement – Part 1: Determination of Strength* (in Portuguese), Comité Européen de Normalisation, Brussels, Belgium, https://www.cen.eu

Cyna, H., Schlosser, F., Frank, R., Plumelle, C., Estephan, R., Altmayer, F., Goulesco, N., Juran, I., Maurel, C., Shahrour, I., and Vezole, P., 2004, "Synthèse des Résultats et Recommandations du Projet National sur les Micropieux. FOREVER," *Presses de l'école nationale des Ponts et Chaussées (ENPC)*, Paris, France, pp. 1–347.

El Hadi Drbe, O. and El Naggar, M., 2015, "Axial Monotonic and Cyclic Compression Behavior of Hollow-Bar Micropiles," *Can. Geotech. J.*, Vol. 52, No. 4, pp. 426–441, https://doi.org/10.1139/cgj-2014-0052

El Sharnouby, M. and El Naggar, M., 2011, "Monotonic and Cyclic Axial Full-Scale Testing of Reinforced Helical Pulldown Micropiles," presented at the *2011 Pan-Am CGS Geotechnical Conference*, Toronto, Ontario, Canada, Canadian Geotechnical Society, Richmond, British Columbia, Canada, pp. 1–6.

El Sharnouby, M. and El Naggar, M., 2012, "Field Investigation of Axial Monotonic and Cyclic Performance of Reinforced Helical Pulldown Micropiles," *Can. Geotech. J.*, Vol. 49, No. 5, pp. 560–573, https://doi.org/10.1139/t2012-017

Francis, R., 1997, "Etude du Comportement Mécanique de Micropieux Modèles en Chamber D'étalonnage, Application aux Effets de Groupe," Ph.D. thesis, Presses de l'école nationale des Ponts et Chaussées (ENPC), Paris, France.

Juran, I., Benslimane, A., and Hanna, S., 2001, "Engineering Analysis of Dynamic Behavior of Micropile Systems," *Trans. Res. Rec.*, Vol. 1772, pp. 91–106, https://doi.org/10.3141/1772-11

Juran, I. and Weinstein, P., 2009, "Long-Term Performance Assessment of Micropiles under Monotonic and Cyclic Loading," presented at the *Ninth International Workshop on Micropiles*, London, UK, International Society for Micropiles, Eighty Four, PA - unpublished

Le Kouby, A., 2003, "Etude du Comportement Mécanique de Micropieux sous Chargements Monotones et Cycliques Verticaux, Application aux Effets de Groupe," Ph.D. thesis, Presses de l'école nationale des Ponts et Chaussées (ENPC), Paris, France.

Lizzi, F., 1978, "Reticulated Root Piles to Correct Landslides," presented at the ASCE National Convention, Chicago, IL, ASCE, Reston, VA, pp. 1–25.

LNEC NP-83, 1965, *Solos, Determinação da Densidade das Partículas* (in Portuguese), Laboratório Nacional de Engenharia Civil, Lisbon, Portugal, http://www.lnec.pt/en/

Matos, R., Pinto, P., Rebelo, C., Gervásio, H., and Veljkovic, M., 2016, "Improved Design of Tubular Wind Tower Foundations Using Steel Micropiles," *Struct. Infrastruct. Eng.*, Vol. 12, No. 9, pp. 1038–1050, https://doi.org/10.1080/15732479.2015.1076853

Russo, G., 2004, "Full-Scale Load Tests on Instrumented Micropiles," *Proc. Inst. Civ. Eng. Geotech. Eng.*, Vol. 157, No. 3, pp. 127–135.

Sabatini, P. J., Tanyu, B., Armour, T., Groneck, P., and Keeley, J., 2005, *Micropile Design and Construction (Reference Manual for NHI Course 132078)*, Publication No. FHWA-NHI-05-039, National Highway Institute, Federal Highway Administration, Washington, DC, pp. 1–456.

Schwarz, P., 2000, "Axial Cyclic Loading of Small Diameter Injection Piles in Sand," presented at the *Third International Workshop on Micropiles*, Türkü, Finland, International Society for Micropiles, Eighty Four, PA, pp. 1–7.

Turner, J. and Kulhawy, F., 1990, "Drained Uplift Capacity of Drilled Shafts under Repeated Axial Loading," *J. Geotech. Eng.*, Vol. 116, No. 3, pp. 470–492, https://doi.org/10.1061/(ASCE)0733-9410(1990)116:3(470)

Veludo, J., Dias-da-Costa, D., Júlio, E. N. B. S., and Pinto, P. L., 2012, "Bond Strength of Textured Micropiles Grouted to Concrete Footings," *Eng. Struct.*, Vol. 35, pp. 288–295, https://doi.org/10.1016/j.engstruct.2011.11.012